THE JOURNAL OF BIOLOGICAL CHEMISTRY VOL. 284, NO. 41, pp. 27980–27988, October 9, 2009

Clustering of Neuronal K^+-Cl^- Cotransporters in Lipid Rafts by Tyrosine Phosphorylation*[S]

Received for publication, July 14, 2009, and in revised form, August 11, 2009 Published, JBC Papers in Press, August 13, 2009, DOI 10.1074/jbc.M109.043620

Miho Watanabe[‡], **Hiroaki Wake**[‡§], **Andrew J. Moorhouse**[¶], **and Junichi Nabekura**[‡§‖1]

From the [‡]*Department of Developmental Physiology, National Institute for Physiological Sciences, Okazaki 444-8585, Japan,* [§]*Core Research for the Evolutionary Science and Technology, Japan Science and Technology Corporation, Saitama 333-0012, Japan, the* [¶]*Department of Physiology, School of Medical Sciences, University of New South Wales, Sydney, New South Wales 2052, Australia, and the* [‖]*Department of Physiological Sciences, The Graduate University for Advanced Studies (SOKENDAI), Hayama 240-0193, Japan*

The neuronal K^+-Cl^- cotransporter (KCC2) is a membrane transport protein that extrudes Cl^- from neurons and helps maintain low intracellular [Cl^-] and hyperpolarizing GABAergic synaptic potentials. Depolarizing γ-aminobutyric acid (GABA) responses in neonatal neurons and following various forms of neuronal injury are associated with reduced levels of KCC2 expression. Despite the importance for plasticity of inhibitory transmission, less is known about cellular mechanisms involved in more dynamic changes in KCC2 function. In this study, we investigated the role of tyrosine phosphorylation in KCC2 localization and function in hippocampal neurons and in cultured GT1-7 cells. Mutation to the putative tyrosine phosphorylation site within the long intracellular carboxyl terminus of KCC2(Y1087D) or application of the tyrosine kinase inhibitor genistein shifted the GABA reversal potential (E_{GABA}) to more depolarized values, indicating reduced KCC2 function. This was associated with a change in the expression pattern of KCC2 from a punctate distribution to a more uniform distribution, suggesting that functional tyrosine-phosphorylated KCC2 forms clusters in restricted membrane domains. Sodium vanadate, a tyrosine phosphatase inhibitor, increased the proportion of KCC2 associated with lipid rafts membrane domains. Loss of tyrosine phosphorylation also reduced oligomerization of KCC2. A loss of the punctuate distribution and oligomerization of KCC2 and a more depolarized E_{GABA} were seen when the 28-amino-acid carboxyl terminus of KCC2 was deleted. These results indicate that direct tyrosine phosphorylation of KCC2 results in membrane clusters and functional transport activity, suggesting a mechanism by which intracellular Cl^- concentrations and GABA responses can be rapidly modulated.

The inhibitory neurotransmitters GABA[2] and glycine activate ionotropic Cl^- channels, typically leading to membrane hyperpolarization in the adult central nervous system. The neuronal K^+-Cl^- cotransporter (KCC2) is the principal membrane transport protein that maintains low intracellular [Cl^-] ($[Cl^-]_i$) in mature and healthy neurons to allow such Cl^- influx and hyperpolarization. However, in immature neurons and in neurons following various forms of neuronal injury, $[Cl^-]_i$ is elevated and GABA and glycine can cause membrane depolarization and neuronal excitation (1–3). A reduced expression of KCC2 protein in immature neurons (4) and a decrease of KCC2 expression in response to various pathophysiological conditions, *e.g.* axotomy (5, 6) and global ischemia (7), are primarily responsible for this increased $[Cl^-]_i$ and for the depolarizing GABA response.

In addition to changes in the expression levels of KCC2 protein, the function of KCC2 can be more dynamically and rapidly modulated by the availability of transport substrates and by various forms of kinase activity. Cl^- extrusion is quantitatively regulated by the K^+ driving force across the membrane (8). Protein kinase C can down-regulate both KCC2 function (9) and surface expression (10). Staurosporine, a broad spectrum kinase inhibitor, produces a rapid up-regulation of KCC2 function in immature neurons (11). Brain-type creatinine kinase binding to KCC2 may also regulate its function (12). Finally, WNK3, by interacting with Ste20-related proline-alanine-rich kinase, prevents the cell swelling-induced activation of KCC2 in *Xenopus* oocytes (13, 14).

KCC2 contains one tyrosine protein kinase phosphorylation consensus site (Tyr-1087) within the long carboxyl terminus in the intracellular region (15). Tyr-1087 is not present in KCC1, another family of KCCs, suggesting that direct tyrosine phosphorylation may uniquely regulate KCC2. The receptor tyrosine kinase, IGF-1, and the soluble tyrosine kinase, Src kinase, activate KCC2 during maturation of hippocampal neurons (16). Oxidative stress decreases the tyrosine phosphorylation of KCC2 and reduces KCC2 function (17). However, just how tyrosine phosphorylation regulates KCC2 function under more physiological conditions is unclear, although modulation of KCC2 has important implications for inhibitory synaptic transmission and neuronal excitability. Furthermore, although KCC2 is uniquely expressed in neurons and may be influenced by the neuronal microenvironment, many of the studies on modulation of KCC function have been done in non-neuronal cell lines, *e.g.* HEK293 cells, and *Xenopus* oocytes. In this study, we therefore examined the role and mechanisms of tyrosine phosphorylation in the regulation of KCC2 function in cultured

* This work was supported by Grant-in-Aids for Scientific Research on Priority Areas 19040030 (to M. W.) and 18077009 (to J. N.) and Grant-in-Aids for Young Scientists (B) 21790234 (to M. W.) from The Ministry of Education, Culture, Sports, Science and Technology, Japan and by grants from the Japan Science and Technology Agency and Core Research for the Evolutionary Science and Technology, Japan Science and Technology Corporation (to J. N.).

[S] The on-line version of this article (available at http://www.jbc.org) contains supplemental Fig. 1.

[1] To whom correspondence should be addressed. Tel.: 81-564-55-7851; Fax: 81-564-55-7853; E-mail: nabekura@nips.ac.jp.

[2] The abbreviations used are: GABA, γ-aminobutyric acid; KCC2, K^+-Cl^- cotransporter; WT, wild type; PBS, phosphate-buffered saline; Tfr, transferrin receptor; MeβCD, methyl-β-cyclodextrin; Ω, ohms.

hippocampal neurons and in GT1-7 cells, a brain-derived cell line that possesses many neuronal characteristics but does not express endogenous KCC2 (18, 19) (also, see "Experimental Procedures"). The present study proposes that tyrosine phosphorylation of KCC2 results in clustering within lipid rafts via interactions within the carboxyl terminus of KCC2 and that this clustering results in efficient extrusion of Cl^-.

EXPERIMENTAL PROCEDURES

All relevant experimental protocols were approved by the Ethics Review Committee for Animal Experimentation of the Japanese Physiological Society.

Plasmid Constructs—The plasmid pEGFP-KCC2, containing cDNA encoding rat KCC2 (GenBank™ accession number U55816) subcloned into the enhanced green fluorescent protein pEGFP-C3 vector (Clontech Laboratories, Inc.), was kindly provided by Dr. John A. Payne (University of California, Davis, CA). Point mutations in KCC2 were produced using the Gene Tailor site-directed mutagenesis kit (Invitrogen) according to the manufacturer's protocol. The putative KCC2 tyrosine phosphorylation site in the carboxyl terminus, Tyr-1087, was mutated to aspartate (Y1087D). The carboxyl-terminal deletion of KCC2 ($KCC2_{\Delta 1189-1116}$) was made by EcoRI digestion and religation. Mutations and deletion were confirmed by DNA sequencing.

Primary Hippocampal Cell Cultures and Transfection of GT1-7 Cells—Day 19 embryos were removed from pregnant Wistar rats under ether anesthesia, and their hippocampi were dissected out and dissociated by papain treatment for 20 min at 32 °C before being plated onto polyethyleneimine-coated coverslips or polystyrene plastic culture dishes. The cultures were maintained in Neurobasal medium (Invitrogen) supplemented with B-27 (Invitrogen). Hippocampal neurons at 27–33 days in culture were used for experiments. GT1-7 cells (kindly provided by Dr. R. Weiner, University of California at San Francisco, CA) were cultured in Dulbecco's modified Eagle's medium (Sigma-Aldrich) with 10% fetal bovine serum, 100 units/ml penicillin, 0.1 mg/ml streptomycin, 1 mM sodium pyruvate, 24 mM $NaHCO_3$, and 4 mM L-glutamine. GT1-7 cells possess neuronal characteristics, including expression of neuronal cell markers (neuron-specific enolase, neurofilament, synaptotagmin, synaptobrevin) and the potency to establish perikarya, neurites, and synapse-like connections with adjacent neurons (18, 20). They also express a variety of neuronal ion channels and receptors, including voltage-gated Na^+, K^+, and Ca^{2+} channels (21, 22) and α-amino-3-hydroxy-5-methyl-4-isoxazolepropionic acid and $GABA_A$ receptors (21). However, GT1-7 cells do not express any endogenous KCC2 (Fig. 1*B*). For patch clamp experiments, cells were plated on to poly L-lysine-coated coverslips. GT1-7 cells were transfected with the wild-type (WT) or mutated pEGFP-KCC2 cDNA plasmid using the TransIT-Neural transfection reagent (Mirus Bio LLC, Madison, WI) according to the manufacturer's protocol. Mock-transfected cells were treated with the transfection reagent but with an empty expression vector.

Immunoprecipitation—Cultured hippocampal neurons were lysed using a sonicator in a buffer solution containing 50 mM Tris-HCl, pH 7.5, 150 mM NaCl, 1% Nonidet P40, and 0.5% sodium deoxycholate, supplemented with protease inhibitor mixture (Roche Applied Science, Penzberg, Germany) and phosphatase inhibitor mixture 2 (Sigma-Aldrich). The cell lysates were centrifuged at 12,000 × *g* for 10 min at 4 °C. Immunoprecipitation was performed using the immunoprecipitation kit (Roche Applied Science) according to the manufacturer's protocol. Briefly, the supernatant was precipitated with KCC2 antibody (Upstate Biotechnology, Charlottesville, VA) for 1 h at 4 °C followed by incubation with protein A-Sepharose overnight at 4 °C. The immunoprecipitates were washed in triplicate with the above buffer solution before being diluted in SDS sample buffer and analyzed by SDS-PAGE and Western blotting.

Lipid Raft Preparation—Cultured hippocampal neurons or GT1-7 cells, either control or drug-treated, were solubilized with 2 ml of 0.1–0.3% Triton X-100 in TNE buffer (50 mM Tris-HCl, pH 7.4, 150 mM NaCl, 5 mM EDTA, protease inhibitor, phosphatase inhibitor mixture 2) for 30 min on ice. The extract was adjusted to 40% sucrose and overlaid with 4 ml of 30% sucrose in TNE buffer and 4 ml of 5% sucrose in TNE buffer. The sample was centrifuged at 39,000 rpm for 17 h at 4 °C using a Beckman SW41 rotor. Twelve different density fractions of equal volume were collected from the top of the sample (low density, fraction 1) to the bottom of the sample (high density, fraction 12). Fractions 4 and 5 contained flotillin-1 and were designated as the lipid raft fractions, whereas the denser fractions contained the transferrin receptor (TfR) and were designated as the non-raft fractions (23, 24). To deplete cholesterol, cells were treated with 10 mM methyl-β-cyclodextrin (MeβCD) for 30 min at 37 °C (25). MeβCD, a water-soluble cyclic oligomer that sequesters cholesterol within its hydrophobic core, depletes cholesterol from the plasma membrane and hence disperses lipid rafts. The membrane cholesterol content was measured using an Amplex red cholesterol assay kit (Invitrogen) according to the manufacturer's protocol. The KCC2 band density in the lipid raft fraction was normalized to the total KCC2 band density, which was normalized to the β-actin band.

Cross-linking of Membrane Protein—Cross-linking was performed following the manufacturer's protocol. Briefly, control and drug-treated cultured hippocampal neurons or GT1-7 cells were washed with ice-cold PBS and incubated with covalent cross-linker bis(sulfosuccinimidyl) suberate (Pierce) for 45 min at 4 °C. After quenching the reaction by adding 20 mM Tris-HCl, pH 7.5, cells were washed with PBS and lysed in 1% Triton X-100 in TNE buffer and subjected to immunoblotting.

Cell Surface Biotinylation—Surface biotinylation experiments were performed using a cell surface protein biotinylation and purification kit (Pierce) according to the manufacturer's protocol. Briefly, GT1-7 cells were washed with ice-cold PBS and then labeled with 0.25 mg/ml sulfo-NHS-SS-biotin for 30 min at 4 °C before washing with PBS supplemented with quenching solution to remove excess biotin. The cell lysates were centrifuged (10,000 × *g*, 2 min), the supernatant was isolated with NeutrAvidin gel, and the bound proteins were then eluted with SDS sample buffer (62.5 mM Tris-HCl, pH 6.8, 1% SDS, 10% glycerol) and analyzed by SDS-PAGE and Western blotting.

Immunoblotting—Proteins were separated using 7.5% acrylamide gels by SDS-PAGE. The gels were transferred to an Immobilon-P membrane (Millipore, Bedford, MA). The blots were blocked in 1% bovine serum albumin and incubated overnight with primary antibody at 4 °C. They were then incubated with horseradish peroxidase-conjugated secondary antibody (GE Healthcare UK Ltd., Buckinghamshire, England) for 1 h at room temperature. Enhanced chemiluminescence (ECL, GE Healthcare) exposure on instant film and an ECL mini-camera luminometer were used to visualize labeled protein. The following primary antibodies (and their dilutions) were used: anti-KCC2 (1:1000, Upstate Biotechnology), anti-phosphotyrosine (1:500, Upstate Biotechnology), anti-β-actin (1:10,000, Sigma-Aldrich), anti-flotillin-1 (1:250, Pharmingen), and anti-TfR receptor (1:500, Zymed Laboratories Inc., San Francisco, CA). The optical densities of bands were analyzed with Scion Image software with a gel-plotting macro program. The phosphotyrosine band density was normalized to the KCC2 band density. The total KCC2 band density was normalized to the β-actin band density. Immunoblots were repeated at least three times to ensure the reproducibility of results.

Immunofluorescence Staining—Cultured hippocampal neurons or GT1-7 cells were incubated with or without drugs, as indicated, and fixed with 4% paraformaldehyde in PBS and then permeabilized with 0.3% Triton X-100. The reaction was blocked with 1% normal goat serum and 2% bovine serum albumin. The KCC2 antibody (1:325) was added and incubated overnight at 4 °C. The fluorescent Alexa Fluor-conjugated secondary antibody (1:300, Invitrogen) was then applied for 2 h at room temperature. Coverslips were mounted in PermaFluor aqueous mounting medium (Thermo Shandon, Pittsburgh, PA), and the immunofluorescent images were acquired with a confocal laser scanning microscope (Leica TCS SP2, Wetzlar, Germany). All imaging acquisitions were done blind. The staining intensity of images was quantified using the ImageJ software (National Institutes of Health). Background levels of fluorescence were subtracted from KCC2 immunofluorescence, and puncta were quantified by using a set threshold intensity (26). The numbers of clusters per cell were counted, and data were normalized to control values.

Electrophysiology—Gramicidin-perforated patch clamp recordings were used to measure membrane currents. Ionic currents were recorded and voltages were controlled using a patch clamp amplifier (MultiClamp 700B; Axon Instruments, Sunnyvale, CA). Currents were filtered at 1 kHz, digitized at 4 kHz, and monitored on a pen recorder and recorded on a computer for analysis. Patch pipettes were made of borosilicate glass capillaries and had a resistance of 4–6 MΩ. The pipette solution consisted of 150 mM KCl and 10 mM HEPES (pH 7.2), supplemented with gramicidin. Gramicidin was dissolved in methanol to prepare a stock solution of 10 mg/ml and then diluted to a final concentration of 30 μg/ml in the pipette solution. The gramicidin solution was prepared just before use. The extracellular solution consisted of the following (in mM): 150 NaCl, 3 KCl, 1 $MgCl_2$, 2 $CaCl_2$, 10 glucose, 10 HEPES (pH 7.4). Voltage offsets were nulled before formation of the GΩ seal. After obtaining a GΩ seal with the cell surface by gentle suction, the pipette potential was set to −50 mV, and −10-mV hyperpolarizing step pulses were periodically delivered to monitor the series resistance. The series resistance typically reached a steady level below 20 MΩ within 40 min after making the GΩ seal, and series resistance errors were electronically compensated by 75–80%. In voltage ramp experiments, 300 nM tetrodotoxin was added to the extracellular solution. To measure the reversal potential of the 30 μM GABA-induced current (E_{GABA}), ramp voltage steps from 0 to −100 mV of 2-s duration were applied before and after GABA application. E_{GABA} was estimated by measuring the voltage at which the I-V relationships before and during GABA application intersected. In the absence of significant concentrations of any other permeant anions such as bicarbonate, the GABA responses are mediated primarily by Cl^-. Hence, the intracellular chloride activities can be estimated from E_{GABA} using the Nernst equation and knowing the extracellular chloride activity. Rapid exchange of the external solution (about 20 ms) was performed using a "Y-tube" perfusion system as described previously (27). Recordings were made at room temperature.

Reagents—Genistein, lavendustin A, sodium vanadate, and MeβCD were purchased from Sigma-Aldrich. All drugs were prepared just before use.

Statistics—The results were expressed as the mean ± S.E. The differences were analyzed by paired *t* test or Student's unpaired *t* test. Differences with $p < 0.05$ were considered significant.

RESULTS

Inhibition of KCC2 Tyrosine Phosphorylation Changed the KCC2 Surface Localization Pattern—We first examined the effect of tyrosine kinase inhibition on the cell surface localization of KCC2. Immunocytochemical analysis of control cultured hippocampal neurons showed punctate membrane staining of KCC2, both on the cell body and on the dendrites (Fig. 1*A*, *panels a*, *d*, and *g*). In cells incubated for 15 min with tyrosine kinase inhibitors, genistein (100 μM, Fig. 1*A*, *panels b* and *e*) or lavendustin A (10 μM, Fig. 1*A*, *panel h*), punctate staining was not apparent, indicating the translocation of KCC2 to a more uniform localization. The effects of tyrosine kinase inhibition were reversible, and when cells were incubated with inhibitors and then washed, punctate staining of KCC2 was again observed (Fig. 1*A*, *panels c* and *f*, genistein; Fig. 1*A*, *panel i*, lavendustin A). We similarly examined the localization pattern of KCC2 in GT1-7 cells expressing KCC2 with enhanced green fluorescent protein (EGFP) tagged at the amino terminus. Untransfected or mock transfected GT1-7 cells showed no expression of KCC2 (Fig. 1*B*) nor any immunofluorescent staining (Fig. 1*C*, *panel a*), respectively. In transfected GT1-7 cells, KCC2 expression also showed a punctate distribution (Fig. 1*C*, *panel b*), whereas for cells treated with genistein or lavendustin A, the KCC2 localization pattern was diffuse (Fig. 1*C*, *panels c* and *d*, respectively), similar to that observed for the cultured hippocampal neurons. Genistein had no effect on the total levels of KCC2 expression (supplemental Fig. 1*A*) nor on the total amount of KCC2 expressed on the cell surface (supplemental Fig. 1*B*). These results indicated that tyrosine kinase inhibitors reversibly induced a change in the localization pattern of KCC2 from a punctate to a diffuse distribution and suggest that tyro-

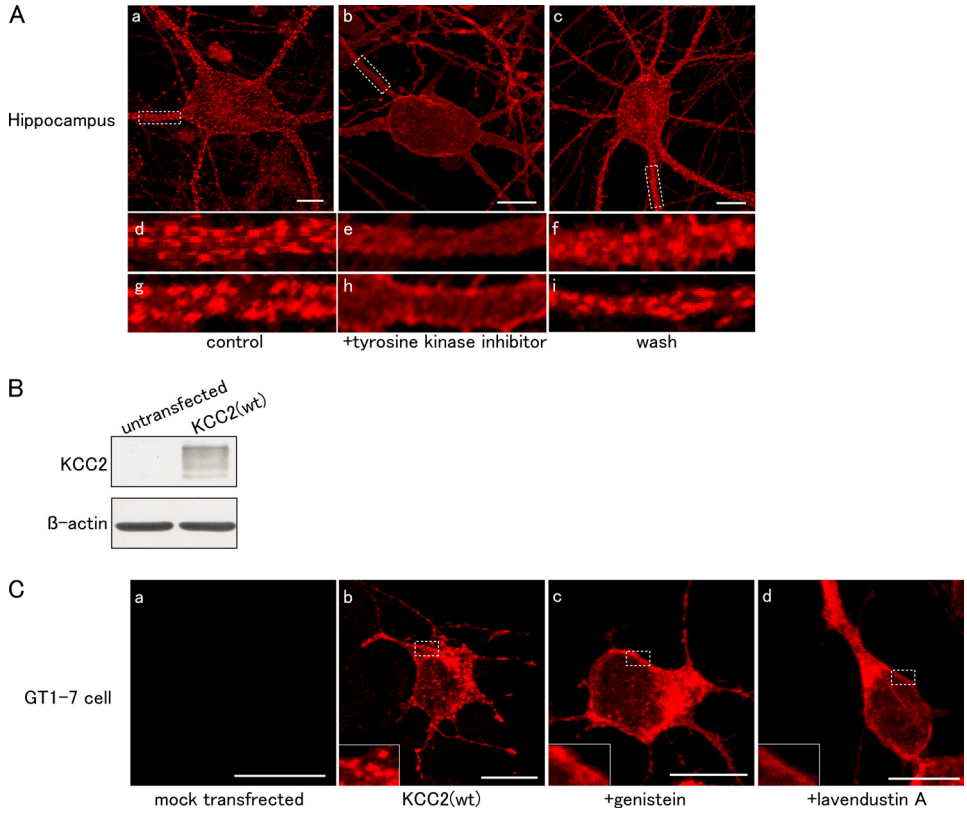

FIGURE 1. **Tyrosine kinase inhibitors reduced the punctate distribution of KCC2.** *A*, confocal microscopic *z*-stacked immunofluorescent images of KCC2 showing punctate staining of KCC2 on the soma and dendrites of a typical cultured hippocampal neuron under control conditions (*panel a*). Fixing neurons after a ~15-min incubation with genistein (100 μM) (*panel b*) resulted in KCC2 immunofluorescence that was less punctate and more diffuse. Following washout of genistein (*panel c*), the more punctate immunofluorescence was restored. *Panels d–f* are magnified views of the *boxed areas* in *panels a–c*. *Panels g–i* are dendrites of another cultured hippocampal neuron under the same conditions as in *panels a–c*, except that the tyrosine kinase inhibitor used in this example was lavendustin A (10 μM). *B*, immunoblot of KCC2 (*upper panel*) or β-actin (*lower panel*) from untransfected GT1-7 cells and GT1-7 cells expressing KCC2(WT). GT1-7 cells had no detectable endogenous KCC2, in contrast to transfected cells. *C*, a similar set of results was observed in GT1-7 cells. *Panels b–d*, confocal microscopic *z*-stacked immunofluorescent images of KCC2 in GT1-7 cells expressing KCC2 under control conditions (*panel b*), after incubation with genistein (*panel c*), and after incubation lavendustin A (*panel d*). No immunofluorescence was observed in GT1-7 cells transfected with the empty expression vector (mock, *panel a*). *Insets* are higher magnification views of the *boxed areas* shown in *panels b–d*. *Scale bar* = 10 μm.

sine-phosphorylated KCC2 forms clusters in a restricted membrane domain.

Inhibition of KCC2 Tyrosine Phosphorylation Resulted in Reduced KCC2 Activity—We next examined the functional consequences of tyrosine kinase inhibition on KCC2 activity. To monitor KCC2 function, we recorded E_{GABA} using gramicidin-perforated patch clamp recordings, which leaves $[Cl^-]_i$ intact (2). We applied 2-s voltage ramps from −100 to 0 mV both before and during application of 30 μM GABA, and E_{GABA} was measured as the voltage at which the two current traces intercepted. Application of genistein to cultured hippocampal neurons shifted E_{GABA} to significantly more depolarized values (Fig. 2, *A* and *B*; by 10.5 ± 1.2 mV, $n = 6$, $p < 0.01$). After washing out genistein, E_{GABA} returned to its control value within about 5 min. The depolarizing shift in E_{GABA} reflected an increase in $[Cl^-]_i$, and we suggest that inhibition of tyrosine kinases reduces Cl^- efflux via a decrease in KCC2 activity.

The altered surface localization and down-regulation of KCC2 function in response to inhibition of tyrosine kinase activity may result from altered phosphorylation of KCC2 itself or of some other modulatory protein. KCC2 does, however, contain a putative tyrosine kinase phosphorylation site located within a hydrophilic domain in the carboxyl terminus (15). To investigate whether KCC2 tyrosine phosphorylation was directly changed, KCC2 was immunoprecipitated from cultured hippocampal neurons with a KCC2 antibody, and the precipitate was subjected to subsequent immunoblot analysis with a phosphotyrosine antibody. Treatment with genistein or lavendustin A reduced the proportion of KCC2 that was tyrosine-phosphorylated to about 40% of the control ratio (Fig. 2*C*, $n = 3$, $p < 0.01$). Thus, the surface translocation of KCC2 was correlated to direct loss of tyrosine phosphorylation of KCC2.

Mutant of Tyrosine 1087 Mimicked the Effects of Tyrosine Kinase Inhibition—The reduced tyrosine phosphorylation of KCC2 presumably related to dephosphorylation at the putative phosphorylation site at Tyr-1087. To more directly test this, we generated single point mutated KCC2 with Tyr-1087 mutated to aspartate (Y1087D) using site-directed mutagenesis (Fig. 3*A*). Both KCC2(WT) and KCC2-(Y1087D) were expressed in GT1-7 cells, and functional analysis was again made using gramicidin-perforated patch clamp recordings. Untransfected GT1-7 cells generated an inward current response to GABA application at a V_H of −50 mV, and E_{GABA} was −36.6 ± 0.9 mV ($n = 5$; Fig. 3*B*). In contrast, in GT1-7 cells expressing KCC2(WT), GABA induced an outward current, which reversed (E_{GABA}) at a significantly more negative potential of −66 ± 2.4 mV ($n = 6$, $p < 0.01$). Furosemide shifted the E_{GABA} to more depolarized values in GT1-7 cells expressing KCC2 (by 12.1 ± 1.4 mV, $n = 6$) but not in untransfected cells. In cells expressing the mutant Y1087D KCC2, GABA induced an inward current at a V_H of −50 mV, and E_{GABA} was the same as in untransfected cells (−36.8 ± 1.1 mV, $n = 8$; Fig. 3*B*). Immunofluorescence analysis that revealed GT1-7 cells expressing KCC2(WT) showed punctate distribution (Fig. 3*C*), as reported above. In contrast, KCC2(Y1087D) showed a more diffuse distribution in the plasma membrane. The number of clusters in KCC2(Y1087D) was reduced to 16.4% of the KCC2(WT) ratio ($p < 0.01$). Thus, the punctate distribution of KCC2 was disrupted by the Y1087D mutation. Together, these results suggest that tyrosine phosphorylation of KCC2 at Tyr-1087 is critical for KCC2 clustering in the plasma membrane. Similar levels of membrane surface-ex-

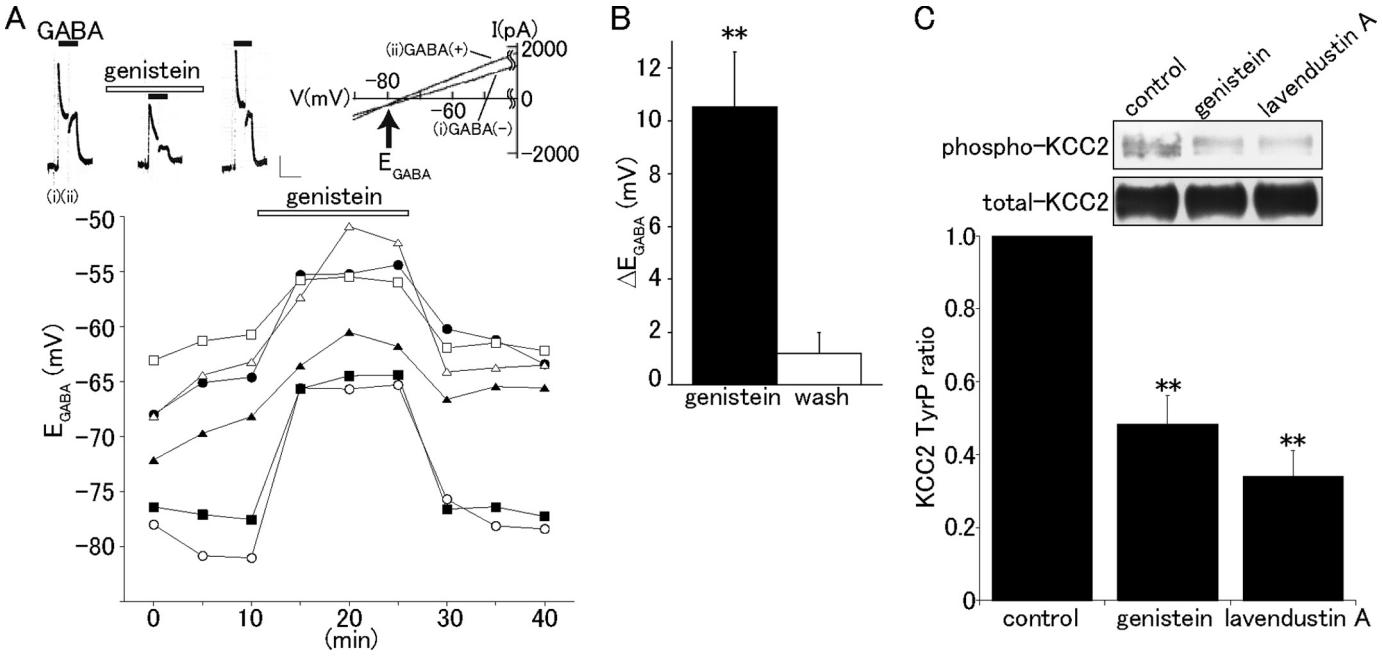

FIGURE 2. **Tyrosine kinase inhibition reduced KCC2 transport function.** *A*, the effect of genistein (100 μM) on E_{GABA} in cultured hippocampal neurons. GABA induced an outward current at $V_H = -50$ mV. After genistein treatment, the amplitude of the GABA current decreased. The *right upper panel* shows sample current-voltage (I-V) curves before and during GABA application; E_{GABA} was estimated by the intersection on the voltage axis of these I-V relationships. The *lower graph* shows the time course of E_{GABA}, before, during, and after genistein treatment, in six separate experiments. Calibrations were: 25 pA, 30 s. *B*, mean maximal E_{GABA} shifts induced by genistein treatment (*black bar*) and following genistein washout (*white bar*) ($n = 6$). Genistein reversibly shifted the E_{GABA} to more depolarized values. *Error bars* indicate S.E. **, $p < 0.01$ *versus* control E_{GABA}. *C*, *upper panel*, sample immunoblots of tyrosine-phosphorylated KCC2 (*phospho-KCC2*) and total KCC2 from the same samples. The bar graph shows a quantitative analysis (densitometric intensity) of the phosphotyrosine (*TyrP*) band (*phospho-KCC2*), normalized to that of KCC2 (total KCC2) and expressed as a percentage of the control value. Genistein ($n = 3$) and lavendustin A ($n = 3$) significantly decreased the proportion of phosphorylated KCC2. **, $p < 0.01$ *versus* control.

pressed KCC2(WT) and Y1087D KCC2 were observed using the biotinylation assay (Fig. 3*D*), indicating that the effects of the Y1087D mutation on KCC2 function and distribution were not due to a reduction in the extent of cell surface expression.

Tyrosine Phosphorylation of KCC2 Facilitated the Association of KCC2 and Lipid Rafts—The above results demonstrate that KCC2 typically shows a punctate membrane distribution that is dependent on tyrosine phosphorylation. Cholesterol/sphingolipid-rich membrane microdomains, so-called lipid rafts, constitute a specialized signaling platform in the plasma membrane, concentrating signaling molecules and pathways that may differ from those found outside such microdomains (28). $GABA_A$ receptors and the Na^+, K^+-ATPase, major components of inhibitory synapses (29), are localized in lipid rafts (30). We therefore investigated whether the punctate distribution of KCC2 in the plasma membrane corresponded to localization in such lipid raft microdomains. Cultured hippocampal neurons were solubilized in 0.1% Triton X-100 at 4 °C and fractionated by discontinuous density gradient and centrifugation (see "Experimental Procedures"). Fractions 4 and 5 contained the highest concentration of cholesterol (Fig. 4*B*) and the lipid raft marker flottilin-1 (Fig. 4*A*) and were hence designated as the lipid raft fractions. Lower density fractions (*fractions 1–3*) contained less cholesterol, whereas the non-lipid raft marker TfR was identified in higher density fractions (*fractions 8–12*), and these were all designated as the non-raft fractions. Immunoblot analysis showed that KCC2 was detectable in the lipid raft fractions (Fig. 4*A*), as well as in the higher density non-raft fractions. We next attempted to confirm the localization of KCC2 in lipid rafts by pharmacological depletion of membrane cholesterol by treatment with MeβCD (25). Treatment with MeβCD totally depleted membranes of cholesterol (Fig. 4*B*) and led to a loss of KCC2 from the lipid raft fractions (Fig. 4*A*). Furthermore, treatment with MeβCD resulted in a more diffuse staining pattern of KCC2 in both hippocampal neurons (*HP*) and GT1-7 cells expressing KCC2(WT) (Fig. 4*C*). These results suggested that some proportion of KCC2 is closely associated with lipid rafts and a punctate distribution. Inhibition of tyrosine phosphatase with sodium vanadate (200 μM) increased the proportion of KCC2 in the lipid raft fractions (Fig. 4*D*, $n = 6$, $p < 0.01$). We also performed lipid raft analysis on the GT1-7 cells transfected with KCC2(WT) and KCC2(Y1087D). More KCC2(WT) was detectable in the lipid raft fraction as compared with mutant KCC2(Y1087D) (Fig. 4*E*). Together, these results indicate that the observed discrete puncta of KCC2 represent a pool of functional KCC2 closely associated with lipid rafts. Furthermore, this lipid raft-associated KCC2 appears to be predominantly tyrosine-phosphorylated.

28 Amino Acids in the Carboxyl Terminus of KCC2 Are Required for Punctate Distribution of KCC2—We next hypothesized that the long carboxyl terminus cytoplasmic tail of KCC2 may play some role in regulation of KCC2 function and distribution. We therefore constructed a KCC2 deletion mutant by deleting the 28 amino acids distal to the tyrosine phosphorylation site (C-$del_{\Delta 1089-1116}$, 1089–1116-amino-acid deletion; Fig. 5*A*). C-$del_{\Delta 1089-1116}$ was expressed in GT1-7 cells, and functional assays were made using gramicidin-perforated patch clamp recordings. In cells expressing KCC2 C-$del_{\Delta 1089-1116}$,

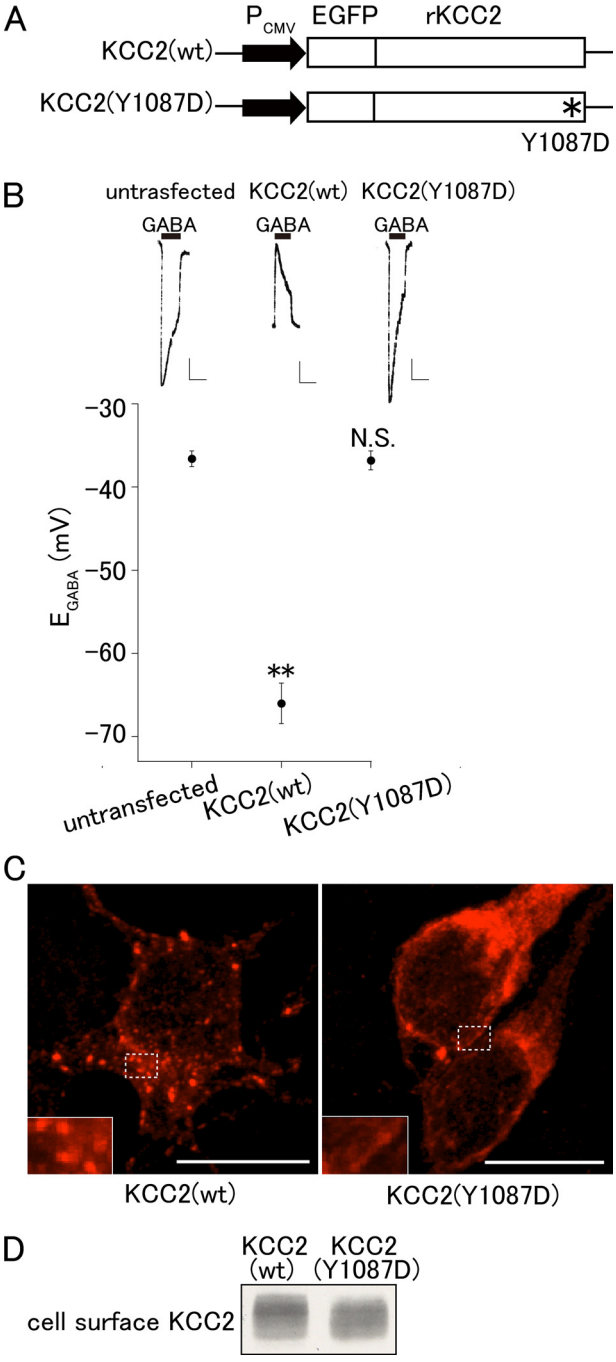

FIGURE 3. **Mutation of the proposed tyrosine phosphorylation motif reduced KCC2 activity and punctate surface distribution.** *A*, schematic diagram of the KCC2(WT) and the KCC2 transfection vector with a tyrosine residue mutated to aspartate (Y1087D). P_{CMV}, cytomegalovirus promoter; *EGFP*, enhanced green fluorescent protein. *B*, GABA induced an inward current in untransfected GT1-7 cells at a V_H of −50 mV. In GT1-7 cells expressing KCC2(WT), GABA induced an outward current, whereas GABA induced an inward current in cells expressing KCC2(Y1087D). Mean E_{GABA} in untransfected GT1-7 cells (control; −36.6 ± 2.1 mV, $n = 5$), in GT1-7 cells expressing KCC2(WT) (−66 ± 5.9 mV, $n = 6$), and in GT1-7 cells expressing KCC2(Y1087D) (−36.8 ± 3.2 mV, $n = 8$) was determined. *Error bars* indicate S.E. **, $p < 0.01$ *versus* untransfected cells. *N.S.*, not significant *versus* untransfected cells. *C*, confocal microscopic *z*-stacked immunofluorescent images of KCC2 in GT1-7 cells expressing KCC2(WT) or the KCC2 Y1087D point mutation. Note a loss of punctate KCC2 staining in KCC2(Y1087D). *Insets* are higher magnification views of the *boxed areas* in the main images. *Scale bar* = 10 μm. *D*, cell surface expression of KCC2 or KCC2(Y1087D) was determined using the biotinylation assay. Sample immunoblots of biotinylated KCC2 in GT1-7 cells expressing KCC2(WT) or KCC2(Y1087D) as indicated. The surface expression of KCC2(Y1087D) was similar to KCC2(WT).

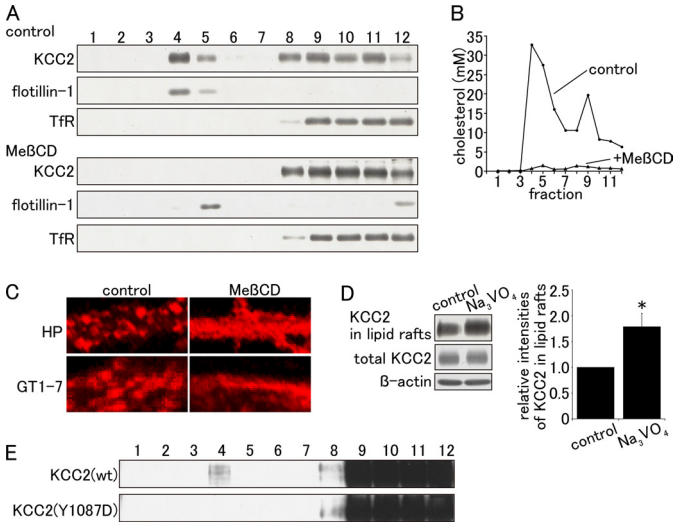

FIGURE 4. **Tyrosine phosphorylation of KCC2 facilitated the association of KCC2 to lipid rafts.** *A*, cultured hippocampal neurons were subjected to sucrose gradient centrifugation after incubation with Triton X-100, and equal volume fractions from low density (*fraction 1*) to high density (*fraction 12*) were isolated and subjected to SDS-PAGE followed by immunoblot using antibodies against KCC2, flotillin-1, and the transferrin receptor (TfR). In control conditions (*upper panel*), KCC2 was detected in the lower density, flotillin-1-enriched fraction (lipid raft fractions 4 and 5). Cholesterol depletion by 10 mM MeβCD pretreatment (*lower panel*) depleted KCC2 from the lipid raft fraction. *B*, graph showing the cholesterol content in the 12 fractions. The lipid raft fractions (fractions 4 and 5) showed the highest concentration of cholesterol. After incubation with MeβCD, there was virtually no cholesterol in any fractions. *C*, confocal *z*-stacked immunofluorescent images of KCC2 showing that MeβCD treatment of hippocampal (*HP*) or GT1-7 cells caused the localization of KCC2 to change from punctate to diffuse. *D*, sample immunoblots of the lipid raft fractions (fractions 4 and 5 in *A* combined). Incubation of neurons with the tyrosine phosphatase inhibitor, sodium vanadate (200 μM), increased the amount of KCC2 in the lipid raft fraction. *Right panel*, quantitative analysis of KCC2 in the lipid raft fraction as a percentage of the control value. Sodium vanadate increased the proportion of KCC2 in the lipid raft fractions to 1.8 ± 0.3 times that of the control ($n = 6$). *Error bars* indicate S.E. *, $p < 0.05$ *versus* control. *E*, GT1-7 cells expressing KCC2(WT) or KCC2(Y1087D) were subjected, as in *A*, to sucrose gradient centrifugation after incubation with Triton X-100, and equal volume fractions from low density (*fraction 1*) to high density (*fraction 12*) were isolated and subjected to SDS-PAGE followed by immunoblot using antibodies against KCC2. More KCC2 (WT, *upper panel*) was detected in the lipid raft fraction as compared with KCC2 (Y1087D, *lower panel*).

E_{GABA} was −36.3 ± 3.4 mV ($n = 6, p < 0.01$), which was similar to E_{GABA} in untransfected cells (Fig. 3*B*), suggesting that C-del$_{\Delta 1089-1116}$ is less potent in keeping E_{GABA} more hyperpolarized. The KCC2 C-del$_{\Delta 1089-1116}$ was still observed to be expressed on the cell membrane surface using the biotinylation assay (Fig. 5*B*). In contrast to the punctate distribution of KCC2(WT) as revealed by immunofluorescence analysis (Figs. 1*C*, *panel b*, 3*C*, and 5*C*), KCC2 C-del$_{\Delta 1089-1116}$ showed a diffuse distribution in the plasma membrane (Fig. 5*C*). The number of clusters in C-del$_{\Delta 1089-1116}$ was reduced to 46.6% of the KCC2(WT) ratio ($p < 0.01$), indicating that the distal carboxyl terminus is required for KCC2 clustering and efficient function.

Loss of Tyrosine Phosphorylation of KCC2 Reduced KCC2 Oligomerization—As the related cation chloride transporters, Na^+-Cl^- transporter (NCC) and Na^+-K^+-$2Cl^-$ cotransporter 2 (NKCC2), form functional dimers (31, 32), and as the oligomerization state of KCC2 increases over development (33), we next asked whether tyrosine phosphorylation changed KCC2 oligomerization. We assessed the oligomerization state of KCC2(WT), KCC2(Y1087D), and KCC2 C-del$_{\Delta 1089-1116}$

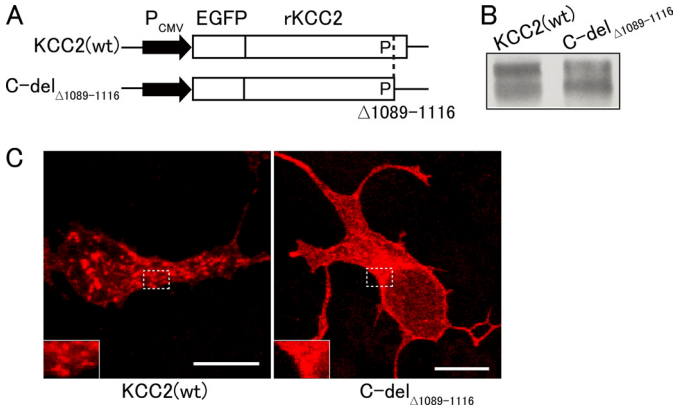

FIGURE 5. **The carboxyl terminus of KCC2 is required for punctate surface distribution of KCC2.** *A*, schematic diagram of the KCC2 deletion mutant vector (C-del$_{\Delta 1089-1116}$) as compared with the KCC2(WT) expression vector. P_{CMV}, cytomegalovirus construct; *EGFP*, enhanced green fluorescent protein. *B*, sample immunoblots of biotinylated KCC2 in GT1-7 cells expressing KCC2(WT) or C-del$_{\Delta 1089-1116}$ as indicated. The surface expression of C-del$_{\Delta 1089-1116}$ KCC2 was similar to that of KCC2(WT). *C*, confocal microscopic *z*-stacked immunofluorescent images of KCC2 in GT1-7 cells expressing KCC2(WT) or C-del$_{\Delta 1089-1116}$ KCC2. Note the loss of punctate KCC2 staining in cells expressing C-del$_{\Delta 1089-1116}$ KCC2. *Insets* are higher magnification views of the *boxed areas* in the main images. *Scale bar* = 10 μm.

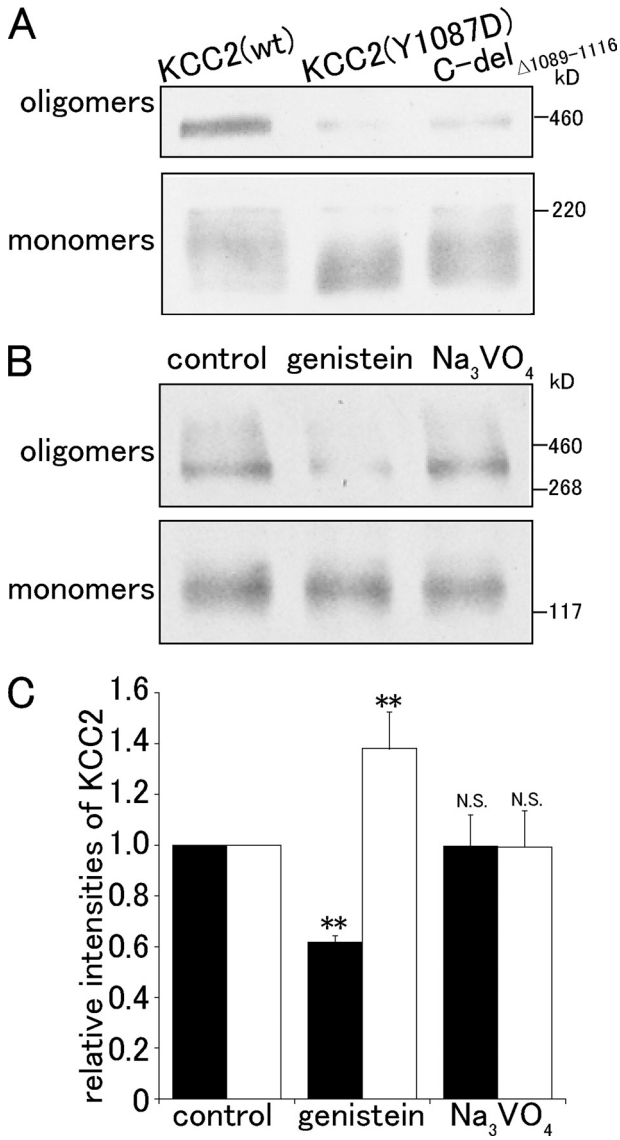

FIGURE 6. **Effects of KCC2 mutations and tyrosine kinase inhibition on KCC2 oligomerization.** *A*, immunoblot analysis of KCC2 from GT1-7 cells expressing KCC2(WT), KCC2(Y1087D), or C-del$_{\Delta 1089-1116}$ KCC2. Oligomers of KCC2(WT) were clearly present, but monomeric KCC2 prevailed in cells expressing KCC2(Y1087D) or C-del$_{\Delta 1089-1116}$ KCC2. *B*, incubation of hippocampal neurons with genistein reduced the level of KCC2 oligomers. Sodium vanadate treatment did not change KCC2 oligomerization. *C*, quantitative analysis of the effects of genistein and sodium vanadate on the intensities of the KCC2 monomer band (*white bars*) and oligomer band (*black bars*), expressed relative to values in control conditions ($n = 3$). *Error bars* indicate S.E. **, $p < 0.01$, *N.S. versus* control.

expressed in GT1-7 cells. Immunoblot analysis showed that KCC2 oligomers were clearly present in cells expressing KCC2(WT), but monomeric KCC2 prevailed in cells expressing KCC2(Y1087D) and C-del$_{\Delta 1089-1116}$ (Fig. 6*A*). Treatment of cultured hippocampal neurons with genistein reduced the proportion of KCC2 oligomers, although no change was seen in response to sodium vanadate (Fig. 6, *B* and *C*, $n = 3$, $p < 0.01$). These results suggest that tyrosine phosphorylation and the carboxyl terminus of KCC2 play a critical role in oligomerization of the KCC2 protein.

DISCUSSION

The main finding of this work is that direct tyrosine phosphorylation of KCC2 is critical for transport function and the membrane localization of KCC2. Tyrosine phosphorylation of KCC2 facilitated both association with lipid rafts into discrete membrane puncta and protein oligomerization, and these involved the carboxyl terminus of KCC2 and phosphorylation of Tyr-1087.

The levels of KCC2 expression and function have a major influence on the transmission of electrical signals at inhibitory synapses. A loss of functional KCC2 transport results in an increase in $[Cl^-]_i$ and a modal shift in GABA- and glycine-mediated responses toward a depolarization. As shown in this study, inhibition of tyrosine phosphorylation and the resultant inhibition of KCC2 function resulted in a positive shift in the equilibrium potential of GABA-mediated responses in both hippocampal neurons and GT1-7 cells. Our recent study in cultured hippocampal neurons reported a loss of tyrosine phosphorylation of KCC2 and a loss of transport function in response to *in vitro* epileptic activity and oxidative stress (17). Our current study indicated that basal tyrosine kinase activity phosphorylates KCC2 and sustains transport function under non-pathological conditions. The generality of our finding extended beyond just cultured hippocampal neurons as tyrosine phosphorylation of KCC2 was also essential for function in the GT1-7 cells.

The punctate distribution of KCC2 indicates a restricted localization to specific microdomains in the plasma membrane. Treatments that disrupted this punctate pattern, including agents such as MeβCD, which are known to disrupt lipid rafts, were associated with reduced transport function. Furthermore, KCC2 was detected in the membrane fractions corresponding to lipid rafts, and the extent of KCC2 found within these raft fractions was enhanced by tyrosine phosphorylation. The function of numerous membrane receptors and transporters are dependent on, or mod-

ified by, localization within lipid rafts (34), and we would propose that KCC2 functions most efficiently when tyrosine-phosphorylated and localized within lipid rafts. A number of proteins involved in synaptic transmission are localized to lipid rafts at postsynaptic synapses. The localization of $GABA_A$ receptors into numerous punctate clusters at inhibitory synapses, for example, is abolished when lipid rafts are disrupted (35). Co-localization of functional KCC2 and GABA receptors within lipid rafts at inhibitory synapses may enable more efficient inhibitory signaling. We have also demonstrated that tyrosine phosphorylation was critical for KCC2 oligomerization. Inhibition of tyrosine kinase or mutation of the tyrosine kinase phosphorylation site (Y1087D) reduced oligomerization. Other members of the cation chloride cotransporter family have also been reported to exist as oligomers; NCC (31), NKCC1 (36), NKCC2 (32), KCC1, and KCC3 (37) all seem to function as homooligomers. In addition, an age-dependent increase in KCC2 oligomerization throughout the nervous system has been reported (33), consistent with the developmental increase in KCC2 function. Hence, we suggest that tyrosine phosphorylation results in localization of KCC2 to lipid rafts, enhances oligomerization, and enhances function.

Deletion of the 28 amino acid residues in the carboxyl terminus of KCC2 prevented the ability of KCC2 to form both punctate clusters and oligomers. This deletion is distal to the tyrosine phosphorylation site at Tyr-1087. One possibility is that tyrosine phosphorylation initiates carboxyl terminus interactions with accessory proteins involved in clustering or anchoring within lipid rafts. The yeast two-hybrid model identified protein associated with Myc (PAM) and brain-type creatine kinase (CKB) as KCC2 binding proteins (38, 39), and KCC2 might interact with these or other unidentified proteins.

In conclusion, we demonstrate that tyrosine phosphorylation of Tyr-1087 results in association of KCC2 within lipid rafts and oligomerization, which confers efficient transport function. Localization of KCC2 may enable rapid control of local $[Cl^-]_i$ at inhibitory synapses. In healthy adult neurons, $[Cl^-]_i$ is low, and GABA induces neuronal hyperpolarization. Changes in KCC2 expression levels during development or in response to injury modulate the effectiveness of GABAergic inhibition (4, 5). More rapid pathological or activity-dependent changes in KCC2 function can also modulate GABAergic inhibitory transmission (9, 17, 40). We propose here a mechanism by which phosphorylation can lead to rapid changes in KCC2 function. Understanding the cellular and molecular mechanisms that modulate KCC2 function may have important implications for the understanding of neurodevelopment and plasticity and provide avenues for novel treatments of brain dysfunction.

Acknowledgments—We are grateful to Dr. H. Ishibashi (National Institute for Physiological Sciences (NIPS)) for excellent technical assistance and helpful discussion and to M. Yoshitomo and T. Ohba (NIPS) for the expert technical assistance.

REFERENCES

1. van den Pol, A. N., Obrietan, K., and Chen, G. (1996) *J. Neurosci.* **16,** 4283–4292
2. Kakazu, Y., Akaike, N., Komiyama, S., and Nabekura, J. (1999) *J. Neurosci.* **19,** 2843–2851
3. Ben-Ari, Y. (2002) *Nat. Rev. Neurosci.* **3,** 728–739
4. Rivera, C., Voipio, J., Payne, J. A., Ruusuvuori, E., Lahtinen, H., Lamsa, K., Pirvola, U., Saarma, M., and Kaila, K. (1999) *Nature* **397,** 251–255
5. Nabekura, J., Ueno, T., Okabe, A., Furuta, A., Iwaki, T., Shimizu-Okabe, C., Fukuda, A., and Akaike, N. (2002) *J. Neurosci.* **22,** 4412–4417
6. Toyoda, H., Ohno, K., Yamada, J., Ikeda, M., Okabe, A., Sato, K., Hashimoto, K., and Fukuda, A. (2003) *J. Neurophysiol.* **89,** 1353–1362
7. Reid, K. H., Guo, S. Z., and Iyer, V. G. (2000) *Brain Res.* **864,** 134–137
8. Kakazu, Y., Uchida, S., Nakagawa, T., Akaike, N., and Nabekura, J. (2000) *J. Neurophysiol.* **84,** 281–288
9. Fiumelli, H., Cancedda, L., and Poo, M. M. (2005) *Neuron* **48,** 773–786
10. Lee, H. H., Walker, J. A., Williams, J. R., Goodier, R. J., Payne, J. A., and Moss, S. J. (2007) *J. Biol. Chem.* **282,** 29777–29784
11. Khirug, S., Huttu, K., Ludwig, A., Smirnov, S., Voipio, J., Rivera, C., Kaila, K., and Khiroug, L. (2005) *Eur. J. Neurosci.* **21,** 899–904
12. Inoue, K., Yamada, J., Ueno, S., and Fukuda, A. (2006) *J. Neurochem.* **96,** 598–608
13. Kahle, K. T., Rinehart, J., de Los Heros, P., Louvi, A., Meade, P., Vazquez, N., Hebert, S. C., Gamba, G., Gimenez, I., and Lifton, R. P. (2005) *Proc. Natl. Acad. Sci. U.S.A.* **102,** 16783–16788
14. Gagnon, K. B., England, R., and Delpire, E. (2006) *Am. J. Physiol. Cell Physiol.* **290,** C134–C142
15. Song, L., Mercado, A., Vázquez, N., Xie, Q., Desai, R., George, A. L., Jr., Gamba, G., and Mount, D. B. (2002) *Brain Res. Mol. Brain Res.* **103,** 91–105
16. Kelsch, W., Hormuzdi, S., Straube, E., Lewen, A., Monyer, H., and Misgeld, U. (2001) *J. Neurosci.* **21,** 8339–8347
17. Wake, H., Watanabe, M., Moorhouse, A. J., Kanematsu, T., Horibe, S., Matsukawa, N., Asai, K., Ojika, K., Hirata, M., and Nabekura, J. (2007) *J. Neurosci.* **27,** 1642–1650
18. Mellon, P. L., Windle, J. J., Goldsmith, P. C., Padula, C. A., Roberts, J. L., and Weiner, R. I. (1990) *Neuron* **5,** 1–10
19. Williams, J. R., Sharp, J. W., Kumari, V. G., Wilson, M., and Payne, J. A. (1999) *J. Biol. Chem.* **274,** 12656–12664
20. Wetsel, W. C., Valença, M. M., Merchenthaler, I., Liposits, Z., López, F. J., Weiner, R. I., Mellon, P. L., and Negro-Vilar, A. (1992) *Proc. Natl. Acad. Sci. U.S.A.* **89,** 4149–4153
21. Martínez de la Escalera, G., and Clapp, C. (2001) *Arch Med Res.* **32,** 486–498
22. Watanabe, M., Sakuma, Y., and Kato, M. (2004) *Endocrinology* **145,** 2375–2383
23. Suzuki, S., Numakawa, T., Shimazu, K., Koshimizu, H., Hara, T., Hatanaka, H., Mei, L., Lu, B., and Kojima, M. (2004) *J. Cell Biol.* **167,** 1205–1215
24. Davies, A., Douglas, L., Hendrich, J., Wratten, J., Tran Van Minh, A., Foucault, I., Koch, D., Pratt, W. S., Saibil, H. R., and Dolphin, A. C. (2006) *J. Neurosci.* **26,** 8748–8757
25. Xia, F., Gao, X., Kwan, E., Lam, P. P., Chan, L., Sy, K., Sheu, L., Wheeler, M. B., Gaisano, H. Y., and Tsushima, R. G. (2004) *J. Biol. Chem.* **279,** 24685–24691
26. Misonou, H., Mohapatra, D. P., Park, E. W., Leung, V., Zhen, D., Misonou, K., Anderson, A. E., and Trimmer, J. S. (2004) *Nat. Neurosci.* **7,** 711–718
27. Ueno, T., Okabe, A., Akaike, N., Fukuda, A., and Nabekura, J. (2002) *J. Biol. Chem.* **277,** 4945–4950
28. Simons, K., and Toomre, D. (2000) *Nat. Rev. Mol. Cell Biol.* **1,** 31–39
29. Payne, J. A., Rivera, C., Voipio, J., and Kaila, K. (2003) *Trends Neurosci.* **26,** 199–206
30. Dalskov, S. M., Immerdal, L., Niels-Christiansen, L. L., Hansen, G. H., Schousboe, A., and Danielsen, E. M. (2005) *Neurochem Int.* **46,** 489–499
31. de Jong, J. C., Willems, P. H., Mooren, F. J., van den Heuvel, L. P., Knoers, N. V., and Bindels, R. J. (2003) *J. Biol. Chem.* **278,** 24302–24307
32. Starremans, P. G., Kersten, F. F., Van Den Heuvel, L. P., Knoers, N. V., and

Bindels, R. J. (2003) *J. Am Soc. Nephrol.* **14,** 3039–3046
33. Blaesse, P., Guillemin, I., Schindler, J., Schweizer, M., Delpire, E., Khiroug, L., Friauf, E., and Nothwang, H. G. (2006) *J. Neurosci.* **26,** 10407–10419
34. Martens, J. R., O'Connell, K., and Tamkun, M. (2004) *Trends Pharmacol. Sci.* **25,** 16–21
35. Hering, H., Lin, C. C., and Sheng, M. (2003) *J. Neurosci.* **23,** 3262–3271
36. Moore-Hoon, M. L., and Turner, R. J. (2000) *Biochemistry* **39,** 3718–3724
37. Casula, S., Shmukler, B. E., Wilhelm, S., Stuart-Tilley, A. K., Su, W., Chernova, M. N., Brugnara, C., and Alper, S. L. (2001) *J. Biol. Chem.* **276,** 41870–41878
38. Inoue, K., Ueno, S., and Fukuda, A. (2004) *FEBS Lett.* **564,** 131–135
39. Garbarini, N., and Delpire, E. (2008) *Cell Physiol. Biochem.* **22,** 31–44
40. Kitamura, A., Ishibashi, H., Watanabe, M., Takatsuru, Y., Brodwick, M., and Nabekura, J. (2008) *Neurosci Res.* **62,** 270–277